Proceedings of the ASME 2024 Conference on Smart Materials, Adaptive Structures and Intelligent Systems
SMASIS2024
September 9-11, 2024
Atlanta Marriot Buckhead, Atlanta, GA

SMASIS2024-140156

TEMPERATURE-DEPENDENT ACOUSTIC PROPERTIES OF MAGNETOSTRICTIVE IRON-GALLIUM ALLOYS

Aidan Belsher[1], Zhangxian Deng[1,2]

[1]The Department of Mechanical and Biomedical Engineering, Boise State University, Boise, ID
[2]The Center for Advanced Energy Studies, Idaho Falls, ID

ABSTRACT

The precise and continuous measurement of reactor core temperature is crucial for the safe and efficient operation of light water reactors. Current sensor technologies are limited in their capabilities for continuous monitoring, linearity, and multi-location detection. Magnetostrictive materials, which deform in response to magnetic fields or exhibit magnetization variation when stressed, offer a promising solution through ultrasonic waveguide thermometers. This study prototyped a high-temperature and radiation-tolerant UT consisting of a solenoid and a Galfenol waveguide, and quantified its performance as a thermometer up to 300 °C. The impact of waveguide diameter, ambient temperature, and thermal treatment on UT performance was then thoroughly assessed. Galfenol waveguides with diameters of 0.5 mm, 0.8 mm, and 1.0 mm showed uniform temperature-dependent behavior with minimal hysteresis error when cycled between RT and 300 °C. The acoustic attenuation coefficient decreased with increasing wire diameter, likely due to the combined effects of eddy currents and magneto-mechanical energy conversion. Although thermal annealing at 900 °C for an hour in a nitrogen environment caused significant surface damage to the waveguides, it effectively relieved internal stress, thus minimizing the nonlinearity in the acoustic attenuation coefficient.

Keywords: Magnetostriction; ultrasonic transducer, iron-gallium alloys

NOMENCLATURE

AC	Alternating Current
DC	Direct Current
Galfenol	Iron-Gallium Alloys
MIMS	Metal Mineral Insulated Metal Sheathed
ppm	Part Per Million
RT	Room Temperature
ToF	Time of Flight
UT	Ultrasonic Transducer

1. INTRODUCTION

Precise and continuous measurement of core temperature is crucial for the safe and efficient functioning of nuclear reactors. For example, in pressurized water reactors, which are among the most widespread types of commercial nuclear reactors, maintaining a high core temperature is essential for maximizing thermal efficiency. However, excessively high core temperatures can cause reactor overheating and potentially lead to catastrophic outcomes, as witnessed in the Three Mile Island incident in 1979, the Chernobyl disaster in 1986, and the Fukushima Daiichi nuclear disaster in 2011.

Current sensor technologies, such as thermocouples and linear variable differential transformers, often fall short in delivering high linearity, continuity, or the capability for multi-location temperature sensing. An emerging solution is the ultrasonic waveguide thermometer, which comprises refractory metal waveguides and UTs. However, traditional piezoelectric UTs, typically made from materials like zinc oxide, aluminum nitride, or lithium niobate, are not ideal due to their lack of durability, weak piezoelectric coupling, and rapid degradation in the harsh conditions of nuclear reactors. Additionally, the integration of piezoelectric ceramics with metallic waveguides poses significant technical challenges. Magnetostrictive materials, which deform in response to magnetic fields and show changes in magnetization under mechanical stress, are promising alternatives for UT development. Galfenol are of particular interest due to their significant magnetostriction[1], mechanical robustness[2], rapid response time[3], excellent radiation tolerance[4,5], and ability to withstand high temperatures[4,6]. However, the deployment of Galfenol-based UTs in nuclear reactors has been hindered by insufficient high-fidelity data on their acoustic properties under varying temperatures, specifically regarding the speed of sound (v_s) and the acoustic attenuation coefficient (η).

The speed of sound is dependent on the material's Young's modulus (E). Through either quasi-static thermal-mechanical

testing[6,7] or dynamic modal analysis[8–10], previous studies have reported E of Galfenol from cryogenic temperatures to 300 ℃. These studies suggest that the temperature-dependence of Young's modulus in Galfenol is due to a combination of factors, including inter-atomic force, magneto-mechanical coupling, internal relaxation, and phase transformation. However, these investigations revealed variable responses of Young's modulus and consequently the speed of sound to temperature changes, showing patterns of increase, stability, or decrease as temperature varied. Acoustic attenuation in magnetostrictive materials originates from material hysteresis, eddy currents, anomalous loss, viscous loss, and internal relaxation[9,11]. While earlier research downplayed the impact of hysteresis and eddy currents in Galfenol, suggesting they were negligible[9], more recent findings indicate that these factors become prominent at elevated operating frequencies[12–14]. However, a significant need exists for high-temperature measurements to elucidate the energy dissipation mechanisms in magnetostrictive materials.

This study systematically examined the acoustic properties of magnetostrictive Galfenol waveguides within a temperature range of RT to 300 ℃, aligning with the typical thermal conditions found in the coolant loops of light-water reactors. The study began by constructing a high-temperature UT. It then investigated the influence of the waveguide's size by testing three different diameters. Finally, the study explored how thermal cycling and thermal annealing processes impact the acoustic properties of Galfenol.

2. METHOD

2.1 High-Temperature UT Configuration

A high-temperature and radiation-tolerant UT is prototyped, as shown in Figure 1. It consists of a Galfenol waveguide, a solenoid made of ceramic-coated nickel-clad copper wire, and MIMS cable for data transmission. The original Galfenol wires (Suzhou Xunshi New Material Co., Ltd) have a nominal Ga content of 19 wt.% and are cold-drawn into three different diameters: 1.0 mm, 0.8 mm, and 0.5 mm. Each waveguide with a length of 20 cm is shear cut from the as-purchased wire spool.

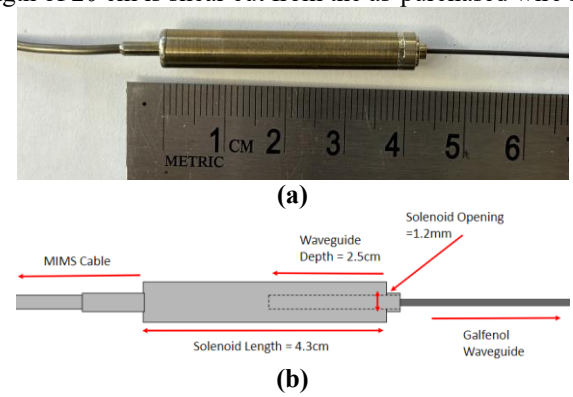

Figure 1: UT physical assembly (a) and schematic (b) consisting of MIMS cable, solenoid, and waveguide.

The solenoid is connected to an ultrasonic pulser/receiver (Ultratek EUT3160) via a MIMS cable. The pulser sends a square voltage wave to the solenoid, transforming the electrical signal into a magnetic pulse. This pulse, through the magneto-mechanical coupling of the Galfenol waveguide, initiates an impulsive acoustic wave. Subsequently, acoustic echoes generate magnetization changes in the waveguide, leading to an electrical voltage across the solenoid by Faraday's law. This voltage is captured by the receiver. The fundamental frequency of the square excitation voltage ranges from 100-130 kHz depending on the waveguide, which aims to match the natural frequency of the waveguide and is selected empirically by maximizing the signal-to-noise ratio.

2.2 Experimental Protocol

The high-temperature UT is then placed in a conventional oven (Faithful WHL-25A), as shown in Figure 2. Preliminary tests indicated that thermocouples in contact with the waveguide have a negligible effect on the ToF measurement but disturb the acoustic damping. Therefore, three Type-K Thermocouples are placed about 1mm away from the waveguide to quantify the temperature gradient during thermal cycling. The UT is tested between RT (20 ℃) and 300 ℃ in 20 ℃ steps. At each interval, UT data is collected 10 minutes after the oven reading stabilizes, resulting in a less than 1 ℃ temperature gradient along the waveguide. For each specified temperature, five datasets are collected to assess the variance in measurements. Each dataset encompasses more than six echoes, enabling the averaging of measurements. All waveguides are tested for at least two heating-cooling cycles at the selected temperature settings.

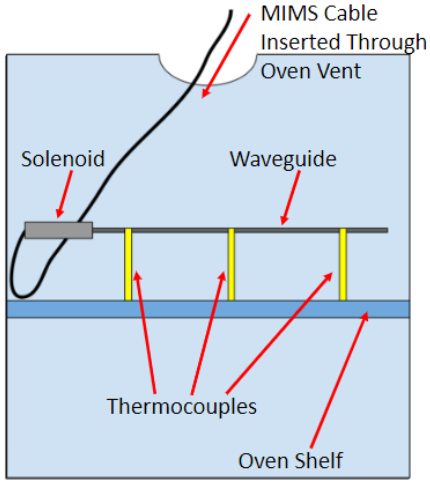

Figure 2: High-temperature UT characterization setup.

2.3 Signal Processing

Figure 3 presents a typical waveform measured from the 0.8 mm diameter waveguide using the pulser/receiver at RT. The ToF between echoes is calculated using the wave interferometer algorithm by cross-correlating the RT and high-temperature signals[15]. This method results in less variances compared to the previous wavelet analysis algorithm[16]. In the wave interferometer analysis, the cross-correlation coefficient CC of the $(i-1)^{th}$ echo signal is

$$CC = \frac{\int_{t_1}^{t_2} S_h^i(t - i\epsilon)\, S_r^i(t)dt}{\int_{t_1}^{t_2} S_h^i(t - i\epsilon)^2\, dt \int_{t_1}^{t_2} S_r^i(t)^2\, dt}$$

Here, subscripts h and r indicate signals at high-temperature and RT, respectively. The time interval $[t_1, t_2]$ is the time window covering the selected echo. The stretching parameter ϵ_{max} that maximizes the cross-correlation coefficient is taken as the ToF value. By using the first four echoes that exhibit reasonable signal-to-noise ratios, both the average value and variance of ToF can be calculated.

The acoustic damping η is derived from the experimental measurement via wavelet analysis[16].

$$\eta = \frac{1}{2(4-i)l_w} \ln\left(\frac{D_i}{D_4}\right)$$

where l_w is the length of the waveguide and D_i is the magnitude of the i^{th} echo obtained from wavelet analysis. Again, the first four echoes are used for damping calculation, enabling data averaging and elucidating measurement variance.

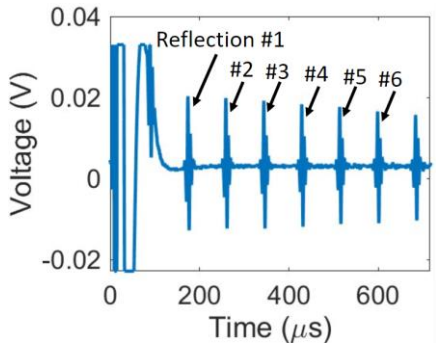

Figure 3: Typical echo waveforms measured from the 0.8 mm diameter waveguide.

3. RESULTS AND DISCUSSION

3.1 Effect of Thermal Cycling

Measurements of time-of-flight (ToF) and the acoustic attenuation coefficient (η) from a newly cut Galfenol waveguide reveal a pronounced phase transformation at 200 °C during the initial heating cycle, as depicted in Figure 4.

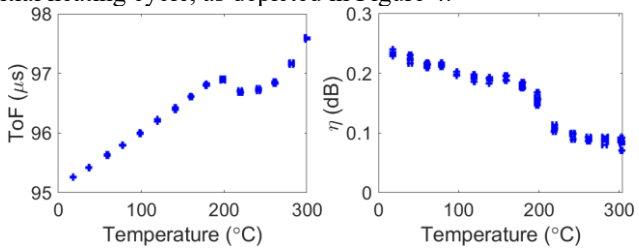

Figure 4: ToF (left) and η (right) of a 0.8mm Galfenol waveguide's first heating cycle.

After the waveguide undergoes a complete thermal cycle from RT to 300 °C, the ToF and η measurements in subsequent thermal cycles exhibit a highly linear and consistent pattern. This consistency suggests that a permanent phase transformation or the alleviation of internal stress takes place at temperatures above 200 °C. Consequently, thermal annealing is crucial for the stable operation of cold-drawn Galfenol waveguides at elevated temperatures. The ToF and η values recorded during the heating phase are virtually identical to those during the cooling phase, as illustrated in Figure 5, leading to a measured maximum hysteresis error of 0.134%.

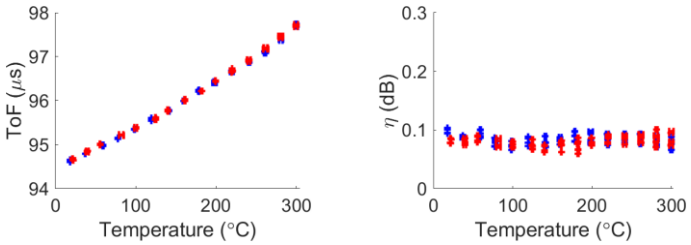

Figure 5: ToF (left) and η (right) of the same 0.8mm waveguide's 2nd heating (blue) and cooling cycle (red).

3.2 Effect of Wire Diameter

The ToF for the 0.8 mm diameter Galfenol waveguide is 14.2% greater than that observed in the other two wires. This particular Galfenol waveguide, sourced from a different batch, suggests that the supplier might have altered the material composition or adjusted the manufacturing processes. Nevertheless, despite these discrepancies, the overall pattern of temperature sensitivity in Galfenol waveguides of different diameters remains consistent, as illustrated in Figure 6.

The thermal sensitivity and acoustic attenuation of the Galfenol waveguide as a thermometer have been quantitatively analyzed, with results presented in Table 1. Sensitivity is determined using the formula:

$$Sen = \frac{\mathrm{ToF}(T) - \mathrm{ToF}(T_0)}{\mathrm{ToF}(T_0)(T - T_0)}$$

where T and T_0 are ambient temperature and RT, respectively. As temperature increases, ToF progressively rises due to the temperature-induced softening of Galfenol. This relationship is characterized by an extremely high correlation coefficient R^2 across all waveguide diameters, highlighting Galfenol's exceptional suitability as a sensing material.

Diameter	Correlation R^2 (ToF)	Correlation R^2 (η)	Sensitivity (ppm/°C)
0.5mm	0.9977	0.0337	124.7887
0.8mm	0.9953	0.1121	114.1236
1.0mm	0.9984	0.0454	123.5888

Table 1: Correlation coefficient R^2 and sensitivity values for each waveguide diameter.

At a given temperature, the value of η decreases with an increase in waveguide diameter. In larger-diameter waveguides, the acoustic energy spreads across a broader cross-sectional area, diminishing the wave's intensity and associated energy loss.

Furthermore, a bigger wire presents a smaller surface-to-volume ratio, which diminishes the likelihood of acoustic energy scattering and absorption at the material's boundaries. However, the temperature dependence of η for a given waveguide diameter demonstrates a low correlation coefficient consistently under 0.115, indicating a nonlinear and inconsistent pattern. This variability is likely attributed to the intricate interaction among anelastic relaxation, eddy currents, and magneto-mechanical coupling.

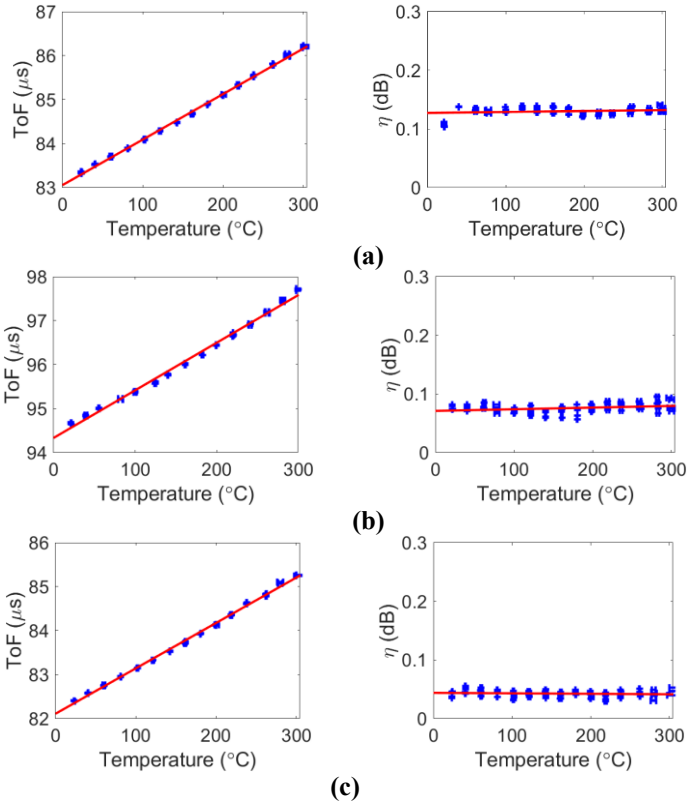

Figure 6: ToF (left) and η (right) versus temperature of 0.5 mm diameter waveguide (a), 0.8 mm waveguide (b) and 1.0 mm waveguide (c).

3.3 Effect of Annealing

Cold-drawn Galfenol waveguide with a 0.8 mm diameter is annealed at 900 °C in N_2 gas atmosphere for one hour to enhance its consistency. Figure 7 illustrates that a crust approximately 0.12 mm thick forms on the surface after annealing. This brittle crust layer readily flakes away, exposing the Galfenol waveguide beneath.

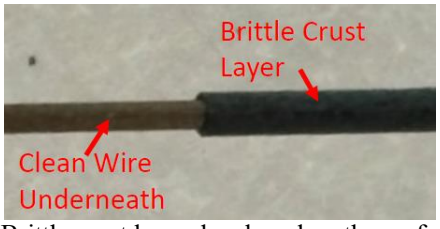

Figure 7: Brittle crust layer developed on the surface of a 0.8 mm-diameter waveguide as a result of annealing.

The ToF for the annealed waveguide maintains similar sensitivity and linearity, whereas the value of η demonstrates a consistent linear decline with rising temperature. The acoustic attenuation coefficient of the annealed waveguide is significantly higher than that of the unannealed counterparts and is on par with values from fresh-cut waveguides. With the resistivity of Galfenol incrementally rising with temperature, the influence of eddy currents and associated energy loss diminishes as temperature escalates. Table 2 showcases that thermal annealing serves as an efficient technique to minimize nonlinearities in acoustic attenuation, concurrently ensuring stability in the ToF measurements.

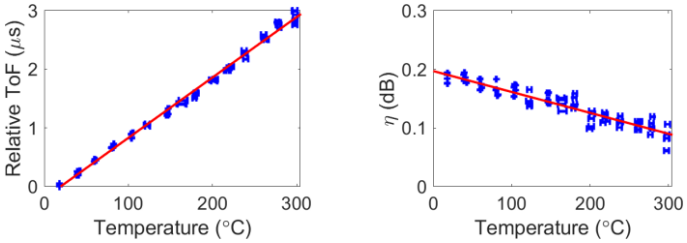

Figure 8: ToF (left) and η (right) of an annealed 0.8mm waveguide.

	R^2 for ToF	R^2 for η	Sensitivity (ppm/°C)
Pre-annealing	0.9953	0.1121	114.1236
Post-annealing	0.9964	0.9624	113.875

Table 2: ToF property comparison of 0.8mm waveguide before and after annealing.

4. CONCLUSION

This study systematically characterized the acoustic properties of magnetostrictive Galfenol waveguides under the actual temperature conditions in light-water reactors. Initially, a high-temperature magnetostrictive UT was developed, incorporating a cold-drawn Galfenol waveguide, a solenoid constructed from ceramic-coated nickel-clad copper wires, and a MIMS cable for transmitting data. Subsequent experiments subjected these Galfenol-based UTs to repeated thermal cycles ranging from room temperature to 300 °C, during which changes in the speed of sound and acoustic attenuation were meticulously documented as a function of the ambient temperature. In addition, the effect of waveguide dimensions was investigated by testing Galfenol waveguides with diameters of 0.5 mm, 0.8 mm, and 1.0 mm. The Galfenol-based UTs exhibited 0.134 % of hysteresis during the thermal cycle. They also achieved a sensitivity of 114.12 to 124.79 ppm/°C and an impressive correlation coefficient above 0.99. During the first heating cycle, each Galfenol waveguide appears to have undergone some thermal annealing, leading to a permanent phase change or loss of internal stress above 200 °C. Subsequent heating cycles achieved the highly linearity, and acoustic attenuation appeared constant with temperature, only decreasing as wire diameter increased This trend in acoustic attenuation is believed to stem

from the interplay between different mechanically-induced eddy currents and anelastic relaxation in each waveguide. Future work will further investigate the effects of thermal annealing on the waveguides using an atmosphere of Ar gas instead of N_2 to avoid potential damage during the annealing process.

The characterization of temperature-dependent acoustic properties from this study offers valuable insights for advancing signal processing techniques and supports the computer-aided design of magnetostrictive guided-wave UTs. These developments are pivotal for enhancing in-pile thermometry and temperature monitoring capabilities within the extreme conditions prevalent in nuclear reactor environments. In addition, new material properties collected in this study will facilitate the development of wireless sensors[17–19] and energy harvesters[12,20,21] that may also operate at high frequencies and elevated temperatures.

ACKNOWLEDGEMENTS

This research was supported by National Aeronautics and Space Administration under Award No 80NSSC22M0172. This work was also prepared as an account of work sponsored by the U.S. Department of Energy, Office of Nuclear Energy Advanced Sensors and Instrumentation program under DOE Idaho Operations Office Contract DE-AC07-05ID14517. Neither the U.S. Government nor any agency thereof, nor any of their employees, makes any warranty, expressed or implied, or assumes any legal liability or responsibility for the accuracy, completeness, or usefulness, of any information, apparatus, product, or process disclosed, or represents that its use would not infringe privately owned rights. References herein to any specific commercial product, process, or service by trade name, trademark, manufacturer, or otherwise, does not necessarily constitute or imply its endorsement, recommendation, or favoring by the U.S. Government or any agency thereof. The views and opinions of authors expressed herein do not necessarily state or reflect those of the U.S. Government or any agency thereof.

REFERENCES

1. Clark, A. E., Restorff, J. B., Wun-Fogle, M., Lograsso, T. A. & Schlagel, D. L. *Magnetostrictive Properties of Body-Centered Cubic Fe-Ga and Fe-Ga-Al Alloys*. *IEEE Transactions on Magnetics* vol. 36 (2000).

2. Nolting, A. E. & Summers, E. Tensile properties of binary and alloyed Galfenol. *J Mater Sci* **50**, 5136–5144 (2015).

3. Ghodsi, M., Modabberifar, M. & Ueno, T. Quality factor, static and dynamic responses of miniature galfenol actuator at wide range of temperature. *International Journal of Physical Sciences* **6**, 8143–8150 (2011).

4. Bowman, C. L. *Design Issues for Using Magnetic Materials in Radiation Environments at Elevated Temperature*. (2013).

5. Reinhardt, B., Daw, J. & Tittmann, B. R. Irradiation Testing of Piezoelectric (Aluminum Nitride, Zinc Oxide, and Bismuth Titanate) and Magnetostrictive Sensors (Remendur and Galfenol). *IEEE Trans Nucl Sci* **65**, 533–538 (2018).

6. Kellogg, R. A., Flatau, A. B., Clark, A. E., Wun-Fogle, M. & Lograsso, T. A. Temperature and stress dependencies of the magnetic and magnetostrictive properties of Fe 0.81Ga 0.19. *J Appl Phys* **91**, 7821–7823 (2002).

7. Kellogg, R. A., Flatau, A., Clark, A. E., Wun-Fogle, M. & Lograsso, T. Quasi-static transduction characterization of Galfenol. in *American Society of Mechanical Engineers, Aerospace Division (Publication) AD* vol. 68 273–280 (American Society of Mechanical Engineers (ASME), 2003).

8. Jen, S. U., Cheng, W. C. & Chiang, F. L. Structural, magneto-mechanical, and damping properties of slowly-cooled polycrystalline Fe81Ga19 alloy. *J Alloys Compd* **651**, 544–550 (2015).

9. Jen, S. U., Lo, Y. Y. & Pai, L. W. Temperature dependence of mechanical properties of the Fe81Ga19 (Galfenol) alloy. *J Phys D Appl Phys* **49**, (2016).

10. Clark, A. E. *et al.* Extraordinary magnetoelasticity and lattice softening in bcc Fe-Ga alloys. in *Journal of Applied Physics* vol. 93 8621–8623 (2003).

11. Ishimoto, M., Numakura, H. & Wuttig, M. Magnetoelastic damping in Fe-Ga solid-solution alloys. *Materials Science and Engineering A* **442**, 195–198 (2006).

12. Deng, Z., Scheidler, J. J., Asnani, V. M. & Dapino, M. J. Shunted magnetostrictive devices in vibration control. *Smart Mater Struct* **29**, (2020).

13. Deng, Z., Zhang, Q. & Dapino, M. J. Dynamic Model for Magnetostrictive Systems with Applications to Damper Design. *IEEE/ASME Transactions on Mechatronics* **23**, 1823–1831 (2018).

14. Scheidler, J. J., Asnani, V. M., Deng, Z. & Dapino, M. J. Dynamic characterization of Galfenol. in *Behavior and Mechanics of Multifunctional Materials and Composites 2015* vol. 9432 94320J (SPIE, 2015).

15. Zhong, B. Measuring Acoustic Nonlinearity of Elastic Materials using Thermal Modulation of Ultrasonic Waves. *PhD Thesis,* University of Nebraska - Lincoln (2022).

16. Keller, A. *et al.* Magnetostrictive Ultrasonic Waveguide Transducer for In-Pile Thermometry. *IEEE/ASME Transactions on Mechatronics* (2022) doi:10.1109/TMECH.2022.3189764.

17. Daw, J., Hone, L. & Woodbury, K. Testing of an Ultrasonic Thermometer Developed at the Idaho National Laboratory. in *Conference Record - IEEE Instrumentation and Measurement Technology Conference* vols 2021-May (Institute of Electrical and Electronics Engineers Inc., 2021).

18. Gao, S., Weng, L., Deng, Z., Wang, B. & Huang, W. Biomimetic tactile sensor array based on magnetostrictive materials. *IEEE Sens J* **21**, 13116–13124 (2021).

19. Shu, L., Yang, J., Li, B., Deng, Z. & Dapino, M. J. Impact force sensing with magnetostrictive Fe-Ga alloys. *Mech Syst Signal Process* **139**, (2020).

20. Deng, Z. & Dapino, M. J. Review of magnetostrictive vibration energy harvesters. *Smart Materials and Structures* vol. 26 Preprint at https://doi.org/10.1088/1361-665X/aa8347 (2017).

21. Dapino, M. J., Deng, Z., Calkins, F. T. & Flatau, A. B. Magnetostrictive Devices. in *Wiley Encyclopedia of Electrical and Electronics Engineering* 1–35 (John Wiley & Sons, Inc., 2016). doi:10.1002/047134608x.w4549.pub2.